Structure Distribution Relationship of Iodine-123-Iodobenzamides as Tracers for the Detection of Melanotic Melanoma

Wolfgang Brandau, Thomas Niehoff, Peter Pulawski, Margot Jonas, Klaus Dutschka, Joachim Sciuk, Heinz H. Coenen and Otmar Schober

Clinic for Nuclear Medicine, Westfälische Wilhelms-Universität Münster, Germany; and Nuclear Chemistry and Radiopharmacy, Clinic for Nuclear Medicine, University of Essen, Germany

The influence of systematic structure variations on the biodistribution of positional isomers of N-(N'-dialkylaminoethylene)-[^{123}I]iodobenzamide (ABA) derivatives in melanoma-bearing animals was investigated. **Methods:** Radioiodination of six bromo benzamide precursors was achieved by Cu(I)-assisted nonisotopic halogen exchange. Organ distribution, scintigraphic and metabolic studies were performed in nude mice bearing a human melanotic MM (SK-MEL 25). A patient suffering from melanotic melanoma underwent scintigraphy with a [^{123}I]iodobenzamide. **Results:** High radiochemical yields of 80%–95% and specific activities of >5 TBq/μmole were obtained. Animal studies revealed specific tumor uptake of all compounds with longest retention of the most lipophilic derivative *p*-[^{123}I]ABA 2-2. At shorter times, however, *o*-[^{123}I]ABA 2-2 exhibited the highest tumor uptake (8.9% ID/g, 1 hr p.i., 10.9% ID/g, 4 hr p.i.). Metabolization of *o*-[^{123}I]ABA 2-2, mainly to *o*-[^{123}I]iodohippuric acid (OIH), followed by fast renal excretion of the metabolites lead to tumor/nontumor ratios (T/NT) of >400 for tumor/blood, and >70 for tumor/liver at 48 h p.i. Unknown metastases could be localized in a patient using *o*-[^{123}I]ABA 2-2. **Conclusion:** The effects of the structure variation of iodobenzamides on their lipophilicity, metabolism and thus pharmacokinetics lead to the suggestion of *o*-[^{123}I]ABA 2-2 as a favorable melanoma imaging agent.

Key Words: melanoma; tumor imaging; iodine-123-iodobenzamides; nonisotopic exchange

J Nucl Med 1996; 37:1865–1871

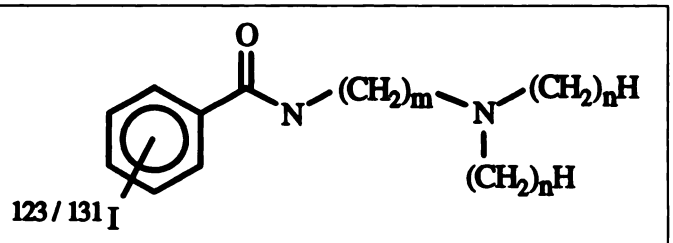

compound	m	n	isomer
o-ABA 2-1	2	1	*ortho-*
m-ABA 2-1	2	1	*meta-*
p-ABA 2-1	2	1	*para-*
o-ABA 2-2	2	2	*ortho-*
m-ABA 2-2	2	2	*meta-*
p-ABA 2-2	2	2	*para-*

FIGURE 1. Structure of aminoalkyl-iodobenzamides.

Although only 3% of malignant skin lesions are related to malignant melanoma, nearly all deaths caused by tumorous skin lesions result from malignant melanoma. The incidence of malignant melanoma ranges from 5 to 10 cases per 100,000 inhabitants per year in northern countries to >30 cases per 100,000 inhabitants per year in the southern regions of the U.S. or in Australia (*1,2*) with still-increasing numbers. The 10-year survival rate of 90%–97% in Stage I (small primary tumor, no metastases) decreases to only 3% in Stage IV (distant metastases) (*3,4*). Therefore, early diagnosis of malignant melanoma and accurate detection of metastases are of essential importance for further therapeutical procedures and prognosis of the disease.

In addition to standard diagnostic tools, e.g., physical examination, sonography, and radiography, several scintigraphic approaches have been developed for the detection of malignant melanoma and its metastases. The use of radiolabeled monoclonal antibodies that bind specifically to melanoma-associated antigens (*5–7*) has been widely explored.

Numerous attempts have also been made to synthesize low molecular compounds which are involved in the synthesis of melanin either as false precursors (*8*) or as enzyme inhibitors. Following these concepts some authors focussed their interest on amino acids (*9,10*), especially on radioiodinated 3-iodo-α-methyltyrosine as inhibitor of tyrosinase, whereas others evaluated thiouracils labeled either with [^{35}S]sulfur or with iodine isotopes as false precursors (*8,11–13*). Additionally, [^{131}I]iodoquinoline derivatives (*14*), [^{123}I]iodoamphetamine (*15,16*), [^{111}In]indiumporphyrine (*17*), [^{57}Co]cobaltbleomycine (*18*) and *m*-[^{131}I]iodobenzylguanidine (*19*) have been evaluated as melanoma imaging agents. Although investigation in animals showed high accumulation of some of these compounds in experimental tumors, none of these derivatives has achieved clinical importance so far, mainly due to unsuitable biokinetics in humans.

Recently, a series of radioiodinated benzamides has appeared to be promising agents for the scintigraphic detection of malignant melanoma (*20,21*). Techniques for their labeling have been improved (*22–24*), and one of these compounds, N-(2-diethylaminoethyl)-4-[^{123}I]iodobenzamide (*p*-[^{123}I]ABA 2-2), has been evaluated in patients with malignant melanoma (*22,25*).

Other radioiodinated, aminoalkylated benzamides have been tested in animals (*26,27*) and a commercially available benz-

Received Nov. 13, 1995; revision accepted Apr. 3, 1996.

For correspondence or reprints contact: Wolfgang Brandau, PhD, Clinic for Nuclear Medicine, Westfälische Wilhelms-Universität Münster, Albert-Schweitzer-Straße 33, D-48129 Münster, Germany

TABLE 1
Biodistribution of *o*-, *m*- and *p*-[^{123}I]ABA 2-1 in Human-Melanoma-Bearing Nude Mice at Various Times Postinjection (%ID/g; Median and Range, n = 3)

Time	Tumor	Blood	Muscle	Lung	Liver	Kidney
ortho-						
5 min	1.56 (1.34–1.71)	2.00 (1.85–2.02)	2.63 (1.52–2.90)	9.46 (8.86–9.66)	8.50 (7.96–11.27)	9.00 (8.96–9.96)
1 hr	4.81 (4.46–6.09)	0.87 (0.78–0.91)	0.69 (0.67–0.90)	2.11 (1.70–2.26)	1.71 (1.59–2.22)	2.90 (2.25–3.13)
4 hr	2.77 (2.43–3.60)	0.06 (0.06–0.20)	0.09 (0.06–0.12)	0.12 (0.11–0.19)	0.09 (0.08–0.15)	0.14 (0.13–0.24)
24 hr	0.75 (0.68–1.11)	0.01 (0.01–0.02)	0.01 (0.01–0.03)	0.05 (0.01–0.05)	0.03 (0.01–0.03)	0.03 (0.01–0.05)
48 hr	0.15 (0.06–0.22)	0.01 (0.01–0.01)	0.01 (0.01–0.01)	0.01 (0.01–0.01)	0.01 (0.01–0.01)	0.01 (0.01–0.01)
meta-						
5 min	2.46 (1.87–3.53)	1.55 (0.89–1.87)	1.86 (1.07–2.13)	23.34 (8.27–30.34)	3.23 (0.07–13.86)	12.14 (6.66–13.23)
1 hr	3.04 (2.34–3.13)	0.46 (0.33–0.48)	0.44 (0.42–0.63)	1.57 (1.51–1.64)	1.93 (1.70–2.11)	1.60 (1.45–1.82)
4 hr	2.53 (2.26–3.09)	0.09 (0.05–0.11)	0.05 (0.03–0.07)	0.22 (0.15–0.72)	0.70 (0.47–0.81)	0.14 (0.08–0.19)
24 hr	1.32 (1.13–2.07)	0.02 (0.01–0.04)	0.02 (0.01–0.06)	0.05 (0.02–0.16)	0.12 (0.09–0.17)	0.03 (0.02–0.05)
48 hr	0.52 (0.20–0.82)	0.01 (0.01–0.01)	0.01 (0.01–0.02)	0.02 (0.01–0.03)	0.04 (0.03–0.04)	0.03 (0.01–0.04)
para-						
5 min	1.88 (1.75–2.64)	1.72 (1.40–2.08)	1.68 (0.86–1.97)	28.16 (17.13–28.20)	11.92 (10.27–15.72)	11.37 (9.85–15.38)
1 hr	4.67 (4.06–6.29)	0.75 (0.55–0.83)	0.60 (0.58–1.66)	3.00 (2.41–3.65)	2.81 (2.08–3.91)	4.73 (3.82–4.85)
4 hr	4.30 (4.12–5.06)	0.07 (0.05–0.08)	0.05 (0.05–0.05)	0.20 (0.17–0.20)	0.22 (0.18–0.28)	0.24 (0.20–0.24)
24 hr	1.52 (1.48–2.30)	0.02 (0.02–0.02)	0.02 (0.02–0.03)	0.04 (0.01–0.09)	0.04 (0.03–0.05)	0.04 (0.02–0.08)
48 hr	1.31 (1.08–1.67)	0.01 (0.01–0.01)	0.01 (0.01–0.01)	0.02 (0.02–0.03)	0.03 (0.02–0.03)	0.02 (0.02–0.03)

amide, the dopamine D_2 receptor imaging agent [^{123}I]-(S)-IBZM, has also been proposed for melanoma scintigraphy (*28*). Recently, (radioiodinated) benzamides have been proven to be selective monoaminoxidase B inhibitors (*29,30*) and as σ receptor ligands for the imaging of breast cancer (*31,32*).

To improve the biokinetic behavior of benzamides as melanoma imaging agents by systematic structure variation we synthesized five new derivatives (Fig. 1) and determined their biodistribution and metabolism in malignant melanoma-bearing nude mice in comparison to the known *p*-ABA 2-2. Furthermore, the most promising ortho-iodobenzamide-2-2 was applied in a patient suffering from malignant melanoma.

MATERIALS AND METHODS

Labeling

The bromo-precursors have been synthesized by a one-step reaction of the corresponding benzoic acid chlorides with the alkylamino compounds as described for *p*-Br-ABA 2-2 and *p*-I-ABA 2-2 (*22*). Labeling was performed as briefly described: sodium [$^{123/131}$I]iodide in 0.01 *N* NaOH was evaporated to dryness in the presence of $Na_2S_2O_5$. After addition of the respective bromobenzamide and CuCl in acetic acid, the reaction mixture was heated for 10–60 min at 180°C. After cooling and evaporation, the residue was dissolved in 400 μl of ethanol and purified by HPLC as described below. For animal studies, the specific activity was adjusted to 5 GBq/μmole by addition of appropriate amounts of nonisotopic bromo compounds to obtain compatibility to former studies (*22*), while human patients received the radiopharmaceuticals with a specific activity of ~5 TBq/μmole.

HPLC separations were performed using a reversed-phase column fitted with a 20-mm pre-column. The column was eluted isocratically with mixtures of 0.2% aqueous diethylamine and acetonitrile (30:70 v/v or 35:65 v/v) at a flow rate of 1 ml/min. The eluates were monitored with an ultraviolet-detector at 254 nm and a NaI(Tl) scintillation detector, evaporated, dissolved in saline and filtered (0.22 μm).

TABLE 2
Biodistribution of *o*-, *m*- and *p*-[^{123}I]ABA 2-2 in Human-Melanoma-Bearing Nude Mice at Various Times Postinjection (%ID/g; Median and Range, n = 3)

Time	Tumor	Blood	Muscle	Lung	Liver	Kidney
ortho-						
5 min	2.78 (1.58–3.01)	1.48 (1.45–2.43)	3.03 (2.55–3.16)	13.45 (9.72–19.54)	20.00 (9.66–23.02)	11.09 (5.22–15.23)
1 hr	8.94 (8.61–12.99)	1.41 (1.23–1.48)	2.61 (1.78–4.53)	4.09 (3.77–5.25)	6.25 (5.54–8.60)	7.31 (5.55–7.58)
4 hr	10.91 (6.40–13.84)	0.42 (0.30–0.87)	0.32 (0.31–0.47)	0.83 (0.45–0.87)	0.73 (0.49–1.00)	0.71 (0.41–0.92)
24 hr	1.72 (1.37–2.64)	0.01 (0.01–0.01)	0.02 (0.01–0.02)	0.02 (0.02–0.03)	0.03 (0.02–0.04)	0.02 (0.02–0.05)
48 hr	1.78 (0.85–3.11)	0.01 (0.01–0.01)	0.01 (0.01–0.16)	0.01 (0.01–0.06)	0.02 (0.01–0.06)	0.01 (0.01–0.06)
meta-						
5 min	1.35 (1.17–3.14)	0.78 (0.78–0.82)	1.58 (1.24–1.63)	17.28 (15.05–20.15)	14.21 (12.91–20.61)	14.08 (12.23–15.07)
1 hr	4.25 (2.30–4.91)	0.64 (0.57–0.69)	0.86 (0.65–1.13)	3.99 (3.13–4.50)	9.08 (8.95–9.20)	4.28 (3.66–4.41)
4 hr	3.21 (1.95–3.75)	0.21 (0.20–0.35)	0.17 (0.07–0.19)	0.65 (0.29–0.82)	2.93 (2.18–4.90)	0.37 (0.28–0.72)
24 hr	2.13 (1.87–4.56)	0.04 (0.04–0.07)	0.01 (0.01–0.18)	0.03 (0.03–0.28)	0.39 (0.39–0.83)	0.05 (0.05–0.23)
48 hr	2.10 (0.60–2.76)	0.03 (0.02–0.04)	0.02 (0.01–0.03)	0.03 (0.03–0.04)	0.38 (0.12–0.43)	0.05 (0.05–0.06)
para-						
5 min	2.88 (2.67–3.36)	0.85 (0.77–1.11)	1.08 (0.77–1.33)	24.03 (20.15–30.04)	23.70 (17.02–26.30)	13.71 (12.87–17.08)
1 hr	5.32 (4.18–6.23)	0.56 (0.54–0.61)	0.94 (0.86–1.00)	7.23 (6.68–9.31)	17.33 (15.34–18.39)	10.43 (8.26–11.14)
4 hr	7.76 (5.13–8.43)	0.25 (0.23–0.40)	0.35 (0.28–0.37)	2.56 (2.54–2.76)	5.78 (4.13–5.81)	3.29 (2.83–3.32)
24 hr	4.34 (4.10–5.34)	0.01 (0.01–0.02)	0.02 (0.02–0.03)	0.07 (0.05–0.11)	0.48 (0.26–0.66)	0.07 (0.05–0.07)
48 hr	2.52 (1.96–2.93)	0.01 (0.01–0.01)	0.01 (0.01–0.01)	0.03 (0.02–0.04)	0.19 (0.16–0.21)	0.04 (0.02–0.04)

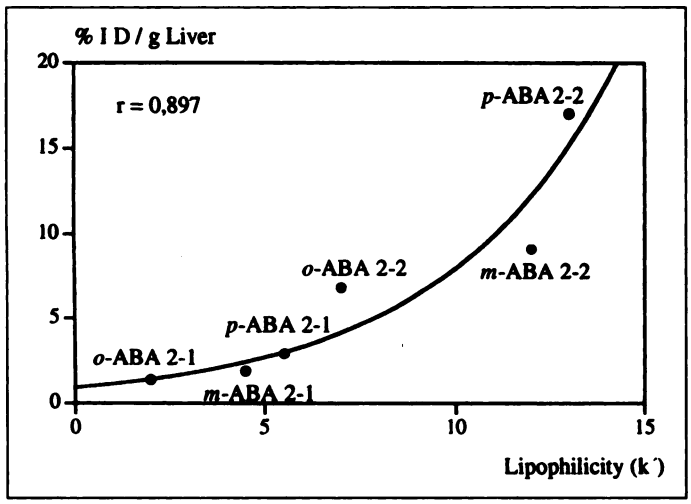

FIGURE 2. Exponential correlation between lipophilicity of the radioiodinated benzamides and liver uptake 1 hr p.i.

Animal Studies

Starting from a stock cell line, human melanotic melanoma cells (SK-MEL 25/P-36/0) were cultured as monolayers for each animal experiment until a cell population of 12×10^6 cells/flask was reached. Culturing conditions were 37°C, 5% CO_2, $NaHCO_3$-RPMI-1640 (5 m*M* HEPES), 15% fetal calf serum, 50.000 units/l penicillin, 50 mg/l streptomycin, and 2 m*M* L-(+)-glutamine. Approximately 1.3×10^7 cells were administered subcutaneously into a flank or into a hind limb of immunodeficient nude mice of 11–13 g body weight. Within 4–5 wk after tumor cell injection 97% of the animals developed well-pigmented nodular melanomas with diameters of 0.25 to 0.6 cm. Histological examination of these tumors revealed the typical characteristics of melanotic melanoma.

For organ distribution studies, 150–180 kBq of the respective [^{123}I]iodinated benzamide in 0.3 ml were injected into a tail vein. At each selected time interval, three animals were killed by cervical dislocation, blood was sampled by cardiac puncture, organs were removed, blotted dry from excess blood, weighed and monitored for radioactivity in an automated well counter. After correction for physical decay the uptake was calculated as percent of the injected dose per gram of organ tissue (% ID/g). Tumor-to-nontumor ratios were calculated as % $ID/g_{tumor}/ID/g_{organ}$. For scintigraphic studies, the administered dose was ~3 MBq per animal and planar scintigrams were obtained under light ether anesthesia at 4 and 24 hr p.i. using a gamma camera fitted with a LEAP collimator because of its higher sensitivity compared to a LEHR collimator. The spatial resolution was about 4 mm at 0 cm distance.

For metabolic studies, urine was collected for 4 hr postinjection of 30 MBq *o*-[^{123}I]ABA 2-2, filtered (0.22 μm) and analyzed by HPLC. *o*-[^{131}I]Iodohippuric acid (OIH) was used as external standard.

The melanin content of the tumor tissue was determined essentially according to a method described in the literature (*33*). The excised tumor samples were stored for 2 mo at −78°C for physical decay of radioactivity. After homogenization and centrifugation, lipids were removed by $CHCl_3$/MeOH and Et_2O/EtOH extractions. Proteins were digested enzymatically by incubation with protease type XIV at 37°C for 48 hr. Melanin was solubilized by addition of 0.1 N NaOH and heating for 48 hr at 120°C and its content was measured by uv absorption at 400 nm. A calibration curve was obtained with synthetic melanin samples which had been dissolved under identical conditions.

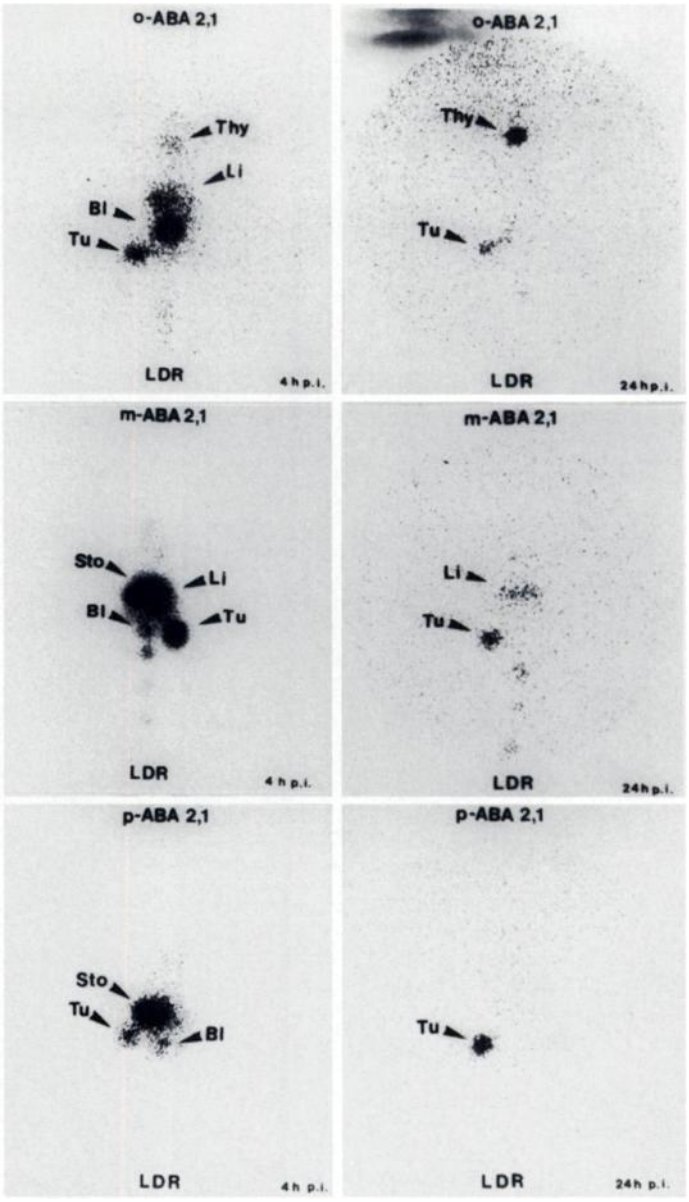

FIGURE 3. Planar images of melanoma-bearing nude mice 4 hr (left column) and 24 hr (right column) after application of *o*-, *m*- and *p*-[^{123}I]ABA 2-1. Tu = tumor; Li = liver; Thy = thyroid; Bl = urinary bladder; Sto = stomach; Co = colon.

Patient Study

The first scintigraphic study using *o*-[^{123}I]ABA 2-2 was performed in a 56-year-old man with metastasized malignant melanoma. His primary tumor had been excised 2 yr before, and liver metastases had been proven by sonography and CT.

The thyroid was blocked with sodium perchlorate prior to application of the radiotracer. After intravenous injection of 150 MBq of *o*-[^{123}I]ABA 2-2, 4 hr p.i. whole-body scans and planar images of the suspected regions were obtained. SPECT studies were performed at 5 hr p.i. using a three-headed gamma camera equipped with medium-energy parallel-hole collimators. Ninety-six projections (32 views/detector, 3.75°/step, non-circular-orbit rotation), each registered over 45 sec were recorded into a 128 × 128 matrix format, corresponding to a pixel dimension of 3.56 × 3.56 mm. System resolution was 12 mm FWHM at 10 cm distance; 100–120 kcts were acquired per view.

Transaxial slices were reconstructed without prefiltering using filtered backprojection with a Butterworth filter of third-order and a cutoff frequency of 0.35 Nyquist. No attenuation correction was

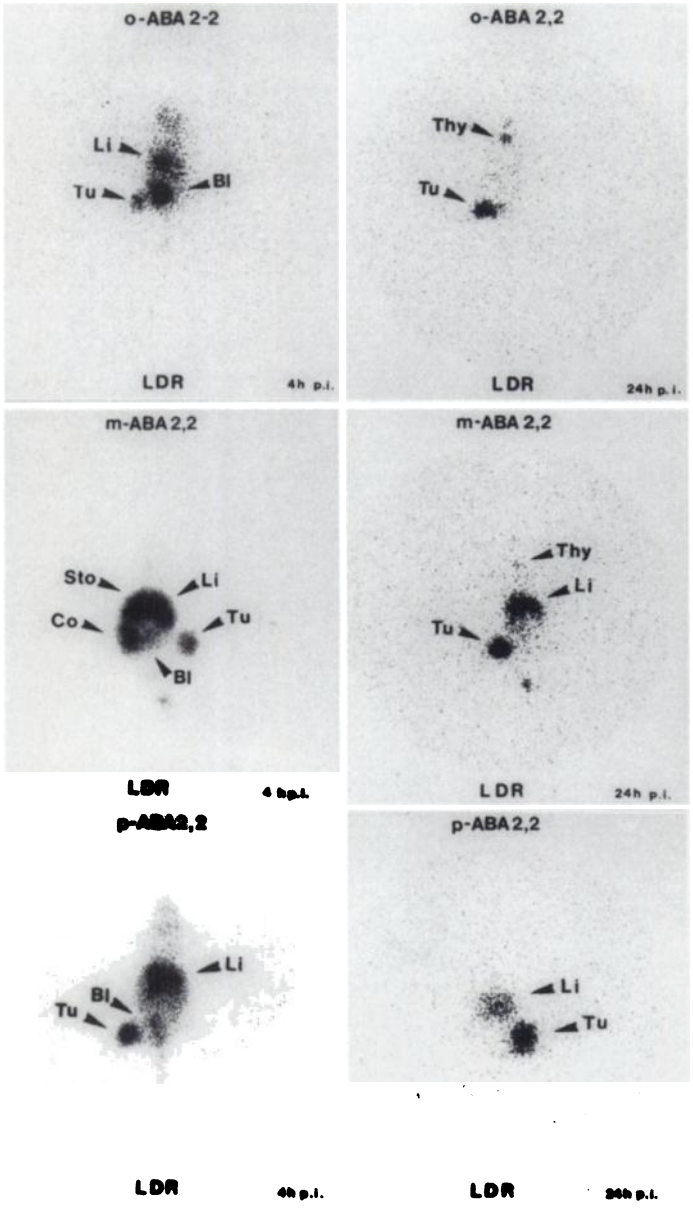

FIGURE 4. Planar images of melanoma-bearing nude mice 4 hr (left column) and 24 hr (right column) after application of *o*-, *m*- and *p*-[^{123}I]ABA 2-2. Tu = tumor; Li = liver; Thy = thyroid; Bl = urinary bladder; Sto = stomach; Co = colon.

performed. In-plane resolution of the reconstructed images was 14 mm FWHM, and slice thickness was approximately 7 mm.

To determine the influence of increased blood flow on tracer accumulation, an additional 30 min dynamic ^{99m}Tc-DTPA study (400 MBq ^{99m}Tc-DTPA) was carried out on the next day. Tumor regions and adjacent lymph nodes were monitored by sonography (7.5 MHz).

The patient's urine was collected up to 4 hr p.i. and analyzed by HPLC (Nucleosil-100, C_{18}, 5 μm, 250 × 4.0 mm, CH_3CN/H_2O/HCOOH 35:65:0.1 (v/v/v), 1.0 ml/min).

RESULTS

Chemistry

All benzamide derivatives could be labeled with radiochemical yields of 80–95% within a total preparation time of 2 hr. Separation of the radioiodinated products from the bromine precursors could be improved compared to former studies (*22*).

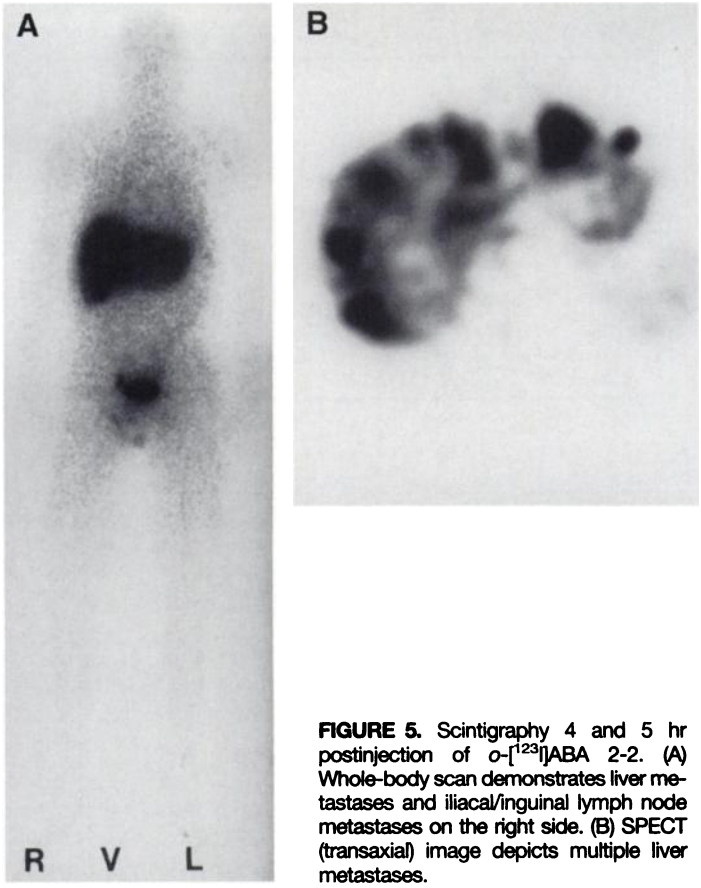

FIGURE 5. Scintigraphy 4 and 5 hr postinjection of *o*-[^{123}I]ABA 2-2. (A) Whole-body scan demonstrates liver metastases and iliacal/inguinal lymph node metastases on the right side. (B) SPECT (transaxial) image depicts multiple liver metastases.

This resulted in the preparation of the radioiodinated benzamides with specific activities of >5 TBq/μmole.

Animal Studies

The melanin content of the tumors was related to the tumor mass with a linear correlation coefficient of r = 0.81 indicating that the human melanoma cell line SK-MEL 25 xenografted into nude mice is a valid model for melanotic malignant melanoma.

The organ distribution of the radioiodinated benzamides is summarized in Tables 1 and 2. Low thyroid uptake (5 min p.i.: <5%, 1 hr p.i.: <0.2%, 48 hr p.i.: <0.1%) reflected the absence of in vivo deiodination. The relatively high values at 5 min p.i. were due to perfusion effects. All compounds showed a distinct tumor accumulation and retention as well as a fast blood clearance. The highest tumor uptake of 10.9% ID/g was observed with *o*-[^{123}I]ABA 2-2 at 4 hr p.i., whereas *p*-[^{123}I]ABA 2-2 exhibited the longest tumor retention (1 hr p.i.: 5.3% ID/g, 4 hr p.i.: 7.8% ID/g, 24 hr p.i.: 4.3%/g). At 1 and 4 hr p.i., significant amounts of extratumoral activity could be detected only in liver and kidneys. Compared to other organs, the tumor uptake was predominant for all ABA-derivatives at times later than 4 hr p.i.

The lipophilicity of the iodobenzamides, as determined by their capacity factors (k′) in HPLC, correlated exponentially with the hepatic uptake at 1 hr p.i. (Fig. 2). In both series of compounds the meta-derivatives showed a less favorable tumor uptake compared to the ortho- and para-derivatives. Scintigraphic studies at 4 and 24 hr p.i. provided a precise delineation of the melanomas from surrounding tissues (Figs. 3, 4). In contrast to the para- and meta-derivatives both ortho-compounds showed a relatively low liver uptake at 4 hr p.i. accompanied by a pronounced renal excretion of radioactivity. Isolation of the animals' urine (performed for *o*-[^{123}I]ABA 2-2)

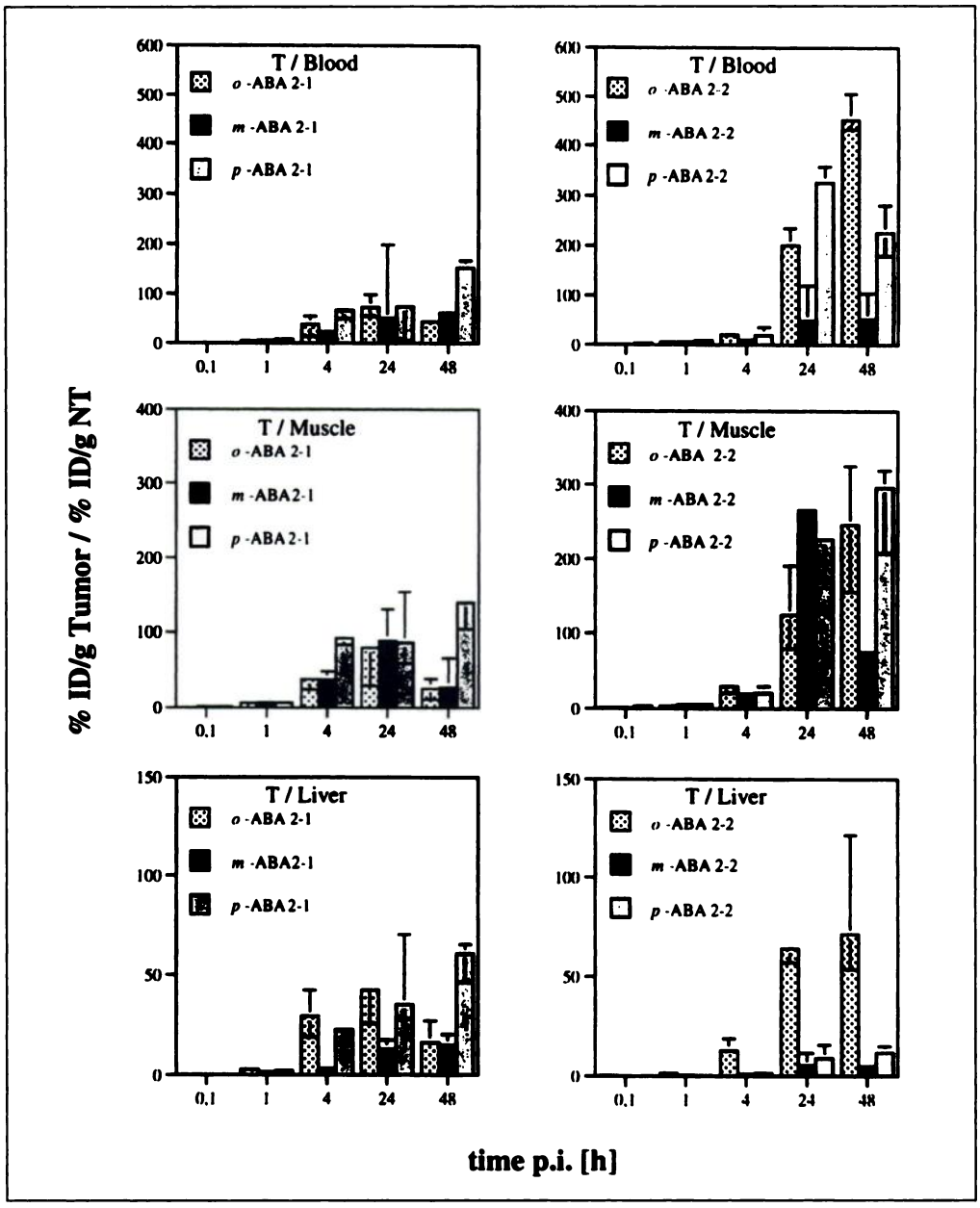

FIGURE 6. Tumor-to-nontumor ratios of *o*-, *m*- and *p*-[^{123}I]ABA 2-1 (left) and *o*-, *m*- and p-[^{123}I]ABA 2-2 (right) in melanoma-bearing nude mice (median and range, n = 3).

TABLE 3
Alterations of the Pharmacokinetic Behavior of *p*-[^{123}I]ABA 2-2 Due to Different Specific Activity and/or Tumor Models

	Time p.i. (hr)	This Work	John et al. (23)	Michelot et al. (21)	Michelot et al. (21)
%ID Tumor	1	5.3	6.1	3.5	6.8
	24	4.3	0.4	0.1	0.7
Tumor-to-Liver	1	0.3	0.5	0.9	1.1
	24	9.0	0.44	0.6	4.9
Tumor-to-Blood	1	9.5	7.9	5.1	6.6
	24	326.7	14.2	6.2	37.3
Tumor-to-Lung	1	0.8	0.8	0.6	0.6
	24	73.8	8.2	1.8	15.8
Tumor model		SK Mel-25	A 2058	M4 Beu	B 16
Origin		human	human	human	murine
Spec. activity (GBq/μmole)		>5	ca. 50	1.3×10^{-3}	1.3×10^{-3}

and subsequent HPLC-analysis revealed that almost 30% of the renally-excreted activity was attributed to ortho-[^{123}I]iodohippuric acid.

Patient Study

Known liver metastases (demonstrated by sonography and CT) were verified by SPECT at 5 hr p.i. (Fig. 5B) and 4 hr p.i. with planar imaging (Fig. 5A), due to the fast clearance of *o*-[^{123}I]ABA 2-2 from normal liver tissue and a prolonged retention in the metastases. In addition, the whole-body scan showed iliacal and inguinal lymph node metastases on the right side. This region was not explorable by radiological imaging following radiation therapy. In the scintigraphic images obtained at 4 hr p.i., considerable amounts of activity were observed in the urinary bladder. HPLC of the urine revealed that approximately 60% of the urinary radioactivity had been excreted as [^{123}I]OIH. An additional perfusion study with ^{99m}Tc-DTPA showed normal distribution of the tracer and gave no evidence for metastatic lesions.

DISCUSSION

Radioiodine-for-bromine exchange followed by HPLC-separation allowed the preparation of 6 radioiodinated benzamides with a very high specific activity of >5 TBq/μmole. All compounds showed good accumulation in experimental melanoma in animals (Tables 1, 2).

High tumor accumulation as well as a fast clearance from other organs at 4 hr p.i. lead to very high tumor/nontumor ratios (Fig. 6, Tables 1, 2). At later times the T/NT-ratios of the meta-isomeres were comparable to those obtained with the ortho- and para-isomeres but the still moderate accumulation of the meta-compounds renders them less appropriate for a potential clinical use. Furthermore, the high activity observed in the stomach with these isomers (Figs. 3, 4) which is difficult to explain, is likely to impair the detection of abdominal lesions. The more lipophilic ortho- and para-2-2 derivatives exhibited maximum tumor uptake at 4 hr p.i., whereas the 2-1 compounds reached their peak value at shorter times (1 hr p.i.). The accumulation of activity in the liver generally rose corresponding to the increasing lipophilicity of the tracer administered (Fig. 2). For nearly all compounds, the T/NT-ratios exceeded unity at 1 hr p.i. except for *p*-[^{123}I]ABA 2-2 and *m*-[^{123}I]ABA 2-2 which exhibited lower tumor-to-liver and tumor-to-kidney ratios at that time.

Tumor-to-blood ratios of up to 67 and tumor/muscle ratios of up to 93 were reached with the more hydrophilic *p*-[^{123}I]ABA 2-1 isomer at 4 hr p.i., whereas the highest ratios by far (tumor-to-blood: 450 for *o*-[^{123}I]ABA 2-2 and tumor-to-muscle: 296 for *p*-[^{123}I]ABA 2-2) were observed at 48 hr after administration of the more lipophilic [^{123}I]ABA 2-2 isomers. The T/NT-ratios depicted in Fig. 6 are the highest ever reported for biodistribution of iodobenzamides and other melanoma-seeking tracers in a mouse tumor model. Comparison with published data revealed similar accumulation of *p*-[^{123}I]ABA 2-2 in different experimental melanoma at 1 hr p.i., but longer tumor retention and corresponding higher T/NT values were found in our tumor model at later times p.i. (Table 3).

At 4 hr p.i., comparison of the ratios found here with those already published for 6 hr p.i. (*34*) indicated only slight differences with regard to *p*-[^{123}I]ABA 2-2. For *o*-[^{123}I]ABA 2-2 and *p*-[^{123}I]ABA 2-1 however, up to seven times higher T/NT-ratios were found with all organs. The lower liver uptake of the hydrophilic [^{123}I]ABA 2-1 compounds resulted in more favorable tumor-to-liver ratios in comparison to the more lipophilic [^{123}I]ABA 2-2 derivatives (Fig. 6). Despite the relatively high lipophilicity of *o*-[^{123}I]ABA 2-2, unexpectedly high tumor-to-liver ratios could be observed for this compound at 24 and 48 hr p.i. This might be explained by the metabolism and pharmacokinetic behaviour of the metabolites. As demonstrated for *o*-[^{123}I]ABA 2-2, the cleavage of the amide-bond followed by conjugation with glycine resulted in ortho-iodohippuric acid which was eliminated renally by tubular excretion. The quick washout of background activity seems to be the main reason for the high T/NT-ratios obtained with the ortho-derivative. Above all, the fast clearance of liver activity could be demonstrated in the animal scintigraphic studies with both ortho-derivatives at 4 hr p.i. (Figs. 3, 4). This advantageous metabolism might only be exploited if iodobenzamides are administered with low mass, i.e., high-specific activity.

The favorable metabolic fate of *o*-[^{123}I]ABA 2-2 could be confirmed in patient studies revealing that 4 hr p.i. almost 60% of radioactivity in the urine had been excreted as OIH. High accumulation in malignant melanoma combined with a fast washout of background activity, particularly from normal liver tissue, provided the scintigraphic detection even of intrahepatic metastases.

Although the uptake mechanisms of benzamides in melanotic melanoma are not understood in detail so far, they inherently will be influenced by several factors, e.g., the tumor model, the specific activity of the administered tracers and, as outlined above, their metabolic fate. The effects due to specific activity are discussed at length in the referenced literature. If a receptor-mediated mechanism is involved in tumor accumulation, as suggested (*26*), highest specific activity of the tracer will be of great importance. This would contradict the results of other authors, who observed significantly increased uptake of radioiodinated benzamides in B16-melanoma along with decreasing specific activity (*27*), and noted the good delineation of tumors in patients using *p*-[^{123}I]ABA 2-2 with quite low specific activity (*25*). Furthermore, preliminary analysis of the melanin content in tumor tissue indicates a correlation with the tracer uptake, a result which is supported by additional cell culture experiments (*35*).

CONCLUSION

Six radioiodinated benzamide derivatives have been synthesized with a high specific activity and evaluated as melanoma imaging agents. Organ distribution studies in melanoma-bearing nude mice revealed high tumor uptake and retention resulting in excellent T/NT-ratios. This metabolic fate could be confirmed in clinical trials leading to a clear detection of multiple hepatic metastases of malignant melanoma. Despite the uncertainties of mechanistic aspects, iodinated benzamides possess great potential for the scintigraphic detection of malignant melanoma.

The favorable metabolism of ortho-derivatives, as demonstrated with *o*-[^{123}I]ABA 2-2, combined with an optimized lipophilicity and specific activity, improves the pharmacokinetic behavior of iodobenzamides as melanoma imaging agents. Further clinical trials and attempts to synthesize other derivatives, which could meet all requirements for routine clinical use, are currently under investigation.

ACKNOWLEDGMENTS

We thank Ms. C. Papenberg for technical assistance, Ms. A. Exler for the scintigraphic studies and Mr. T. Isokeit for figure layout. We also thank Prof. Sorg, Dept. of Experimental Dermatology, University Münster for providing the tumor cell line and Dr. C. Rübe, Clinic for Radiation Therapy, University Münster for providing some of the animals.

REFERENCES

1. Marks R. An overview of skin cancers. *Cancer* 1995;75:607–612.
2. NIH Consensus Conference. Diagnosis and treatment of early melanoma. *JAMA* 1992;268:1314–1319.
3. Orfanos CE, Jong EG, Rassner G, Wolff HH, Garbe C. Stellungnahme und empfehlungen der kommission malignes melanom der Deutschen Dermatologischen Gesellschaft zur diagnostik, behandlung und nachsorge des malignen melanoms der haut: stand 1993/94. *Hautarzt* 1994;45:285–291.
4. Häffner AC, Garbe C, Burg G, Büttner P, Orfanos CE, Rassner G. The prognosis of primary and metastasising melanoma. an evaluation of the TNM classification in 2495 patients. *Br J Cancer* 1992;66:856–861.
5. Buraggi GL, Callegaro L, Mariani G, et al. Imaging with ^{131}I-labeled monoclonal antibodies to a high-molecular-weight melanoma-associated antigen in patients with melanoma: efficacy of whole immunoglobulin and its $F(ab')_2$ fragments. *Cancer Res* 1985;45:3378–3387.
6. Larson S. Biologic characterization of melanoma tumors by antigen-specific targeting of radiolabeled anti-tumor antibodies. *J Nucl Med* 1991;32:287–291.
7. Siccardi AG, Buraggi GL, Natali PG, Scassellati GA, Viale G, Ferrone S and the European Multicenter Study Group. European multicenter study on melanoma immunoscintigraphy by means of ^{99m}Tc-labeled monoclonal antibody fragments. *Eur J Nucl Med* 1990;16:317–323.
8. Dencker L, Larsson B, Olander K, Ullberg S, Yokata M. False precursors of melanin as selective melanoma seekers. *Br J Cancer* 1979;39:449–452.
9. Kloss G, Leven M. Accumulation of radioiodinated tyrosine derivatives in the adrenal medulla and in melanomas. *Eur J Nucl Med* 1979;4:170–186.
10. Bubeck B, Eisenhut M, Heimke U, zum Winkel K. Melanoma affine radiopharmaceuticals. I. A comparative study of ^{131}I-labeled quinoline and tyrosine derivatives. *Eur J Nucl Med* 1981;6:227–233.
11. Fairchild RG, Packer S, Greenberg D, et al. Thiouracil distribution in mice carrying transplantable melanoma. *Cancer Res* 1982;42:5126–5132.
12. Larsson B, Olander K, Dencker L, Holmqvist L. Accumulation of ^{125}I-labeled thiouracil and propylthiouracil in murine melanotic melanomas. *Br J Cancer* 1982; 46:538–550.
13. Coderre JA, Packer S, Fairchild RG, et al. Iodothiouracil as a melanoma localizing agent. *J Nucl Med* 1986;27:1157–1164.
14. Lambrecht RM, Packer S, Wolf AP, Lloyd D, Atkins HL. Detection of ocular melanoma with 4-(3-dimethylamiopropylamino)-7-[^{123}I]-Iodoquinoline. *J Nucl Med* 1984;25:800–804.
15. Ono S, Fukunaga M, Otsuka N, et al. Visualization of ocular melanoma with N-isopropyl-*p*-[^{123}I]-iodoamphetamine. *J Nucl Med* 1988;29:1448–1450.
16. Cohen MB, Saxton RE, Lake RR, et al. Detection of malignant melanoma with iodine-123-iodoamphetamine. *J Nucl Med* 1988;29:1200–1206.
17. Foster N, Woo DV, Kaltovich F, Emrich J, Ljungquist C. Delineation of a transplanted malignant melanoma with indium-111-labeled porphyrin. *J Nucl Med* 1985;26:756–760.
18. Valdés Olmos RA, van der Bergh JHAM, den Hamer JF, Serdjin HJ. Positive ^{57}Co-bleomycin scintigraphy in silent mediastinal metastases of malignant melanoma. *Eur J Nucl Med* 1985;10:86–87.
19. Osei-Bonsu A, Kokoschka EM, Ulrich W, Sinzinger H. Iodine-131-metaiodobenzylguanidine (MIBG) for bronchial oat-cell cancer and melanoma detection? *Eur J Nucl Med* 1989;15:629–631.
20. Michelot J, Veyre A, Bonafous J, et al. Phase II scintigraphic study of malignant melanoma (mm) and metastases with 123-iodine N-(2-diethylaminoethyl) 4-iodbenzamide [Abstract]. *Eur J Nucl Med* 1991;32:547.
21. Michelot JM, Moreau M-FC, Labarre PG, et al. Synthesis and evaluation of new iodine-125 radiopharmaceuticals as potential tracers for malignant melanoma. *J Nucl Med* 1991;32:1573–1580.
22. Brandau W, Kirchner B, Bartenstein B, Sciuk J, Kamanabrou D, Schober O. N-(2-diethylaminoethyl)-4-[^{123}I]iodobenzamide as a tracer for the detection of malignant melanoma: simple synthesis, improved labeling technique and first clinical results. *Eur J Nucl Med* 1993;20:238–243.
23. John CS, Saga C, Kinuya S, et al. An improved synthesis of [^{125}I]N-(diethylaminoethyl)-4-iodobenzamide: a potential ligand for imaging malignant melanoma. *Nucl Med Biol* 1993;20:75–79.
24. Coenen HH, Dutschka KP, Brandau W. N.c.a Cu(I)-assisted iodine-exchange on N-alkylated ortho-, meta- and para-bromo benzamides. *J Lab Compd Radiopharm* 1994;35:222–223.
25. Michelot JM, Moreau MFC, Veyre AJ, et al. Phase II scintigraphic clinical trial of malignant melanoma and metastases with iodine-123-N-(2-Diethylaminoethyl 4-iodobenzamide). *J Nucl Med* 1993;34:1260–1266.
26. John CS, Bowen WD, Saga T, et al. A malignant melanoma imaging agent: synthesis, characterization, in vitro binding and biodistribution of iodine-125-(2-piperidinylaminoethyl)4-iodobenzamide. *J Nucl Med* 1993;34:2169–2175.
27. Nicholl C, Eisenhut M. 4-Jodbenzamide für die Melanomdiagnostik: der Einfluß von Struktur und spezifischer Aktivität auf die Tumoraffinität [Abstract]. *Nuklearmedizin* 1995;34:A110.
28. Maffioli L, Mascheroni L, Mongioj V, et al. Scintigraphic detection of melanoma metastases with a radiolabeled benzamide ([iodine-123]-(S)-IBZM). *J Nucl Med* 1994;35:1741–1747.
29. Raffi H, Chalon S, Ombetta J-E, et al. Synthesis and characterization of [^{125}I]N-(2-aminoethyl)-4-iodobenzamide as a selective monoamine oxidase B inhibitor. *Nucl Med Biol* 1995;22:617–623.
30. Ohmomo Y, Murakami K, Hirata M, et al. Synthesis and evaluation of iodinated benzamide derivatives as selective and reversible monoamine oxidase B inhibitors. *Chem Pharm Bull* 1992;40:1789–1792.
31. John CS, Vilner BJ, Bowen WD. Synthesis and characterization of [^{125}I]-N-(N-Benzylpiperidin-4-yl)-4-iodobenzamide, a new σ receptor radiopharmaceutical: high-affinity binding to MCF-7 breast tumor cells. *J Med Chem* 1994;37:1737–1739.
32. John CS, Vilner BJ, Gulden ME, et al. Synthesis and characterization of [^{125}I]-N-(N-benzylpiperidin-4-yl)-4-iodobenzamide: a high-affinity σ receptor ligand for potential imaging of breast cancer. *Cancer Res* 1995;55:3022–3027.
33. Watts KP, Fairchild RG, Slatkin DN, et al. Melanin content of hamster tissues, human tissues and various melanomas. *Cancer Res* 1981;41:467–472.
34. Moreau MF, Michelot J, Papon J, et al. Synthesis, radiolabeling, and preliminary evaluation in mice of some (N-diethylaminoethyl)-4-iodobenzamide derivatives as melanoma imaging agents. *Nucl Med Biol* 1995;22:737–747.
35. Coenen HH, Brandau W, Dittmann H, et al. Evaluation of melanoma seeking N-(dialkylamino)-alkyl-[^{123,131}I]iodobenzamides by animal and cell-culture studies. *J Lab Compd Radiopharm* 1995;37:260–262.